Korean J. Chem. Eng., **25**(1), 176-180 (2008)

Single-layer organic-light-emitting devices fabricated by screen printing method

Dong-Hyun Lee, Jaesoo Choi, Heeyeop Chae, Chan-Hwa Chung and Sung M. Cho†

Department of Chemical Engineering, Sungkyunkwan University, Suwon 440-746, Korea
(*Received 20 April 2007 • accepted 20 May 2007*)

Abstract−Single-layer organic-light-emitting devices (OLEDs) have been fabricated by screen printing method. Using the screen printing method, a polystyrene (PS) film doped with NPB, Alq_3, and rubrene was deposited to have the thickness of 100 nm. The film was used for the fabrication of single-layer OLEDs. In order to estimate the performance of the devices, single-layer OLEDs of the same structure were also fabricated by spin coating and compared with those fabricated by screen printing. The spin-coated OLEDs were turned on at 10 V and reached a maximum brightness of 1,100 Cd/m^2 at 21 V. The screen-printed OLEDs showed the same turn-on voltage but with a maximum brightness of 110 Cd/m^2 at 14 V.

Key words: Screen Printing, Spin Coating, OLED, Dark Spot

INTRODUCTION

Even though multi-layer organic light emitting devices (OLEDs) have been known to be more efficient than single-layer OLEDs [1,2], the single-layer OLEDs have also attracted attention due to their simple structure. Single-layer OLEDs have mainly been fabricated by spin coating [3,4] of polymeric solutions. In order to increase the emission efficiency of the single layer OLEDs, the phosphorescent OLEDs have been frequently studied by doping a phosphorescent dye in an organic layer [5-7].

Recently, as a new fabrication process of OLEDs, a screen printing process has been exploited [8,9]. Screen printing has been known to be one of the most versatile, simple, fast, cost-effective coating techniques. Not only does it not require expensive vacuum technology, as is the case with physical vapor deposition, but it also can be applied to versatile surface shapes and sizes. Due to its conventional usages, however, it has been believed that screen printing is not suitable for deposition of thin films with less than 100 nm thickness. Pardo et al. [10] demonstrated the use of screen printing in the deposition of an organic active layer having a thickness of several tens of nanometers and acting as a hole-transport layer (HTL) in a multi-layer OLED. Their device emitted light at low voltage (<5 V) and had a peak external quantum efficiency of 0.91%. Although for their device only the HTL was screen-printed while the ETL was deposited by vacuum sublimation, the results were very encouraging since they opened a new possibility that the screen printing process could be utilized for fabricating the OLEDs.

In this study, we fabricated single-layer OLEDs by the screen printing method, and compared the devices were compared single-layer OLEDs fabricated by spin coating. The surface morphology, roughness, and device degradation behavior were directly compared for both OLEDs fabricated by screen printing and spin coating.

EXPERIMENTAL

ITO glasses of a nominal sheet resistance of 30 Ω/□ were ultrasonically cleaned, followed by rinsing with deionized water, trichloroethylene, acetone and methanol. The cleaned ITO glasses were patterned via a standard microlithographic process. HCl (37%, Aldrich) was used as the etchant for the ITO. For the surface treatment of the ITO, the patterned ITO glasses were either treated by oxygen plasma at 100 W for 3 min or spin-coated by PEDOT/PSS film prior to the deposition of OLED active layers.

NPB (N,N'-bis(naphthalen-1-yl)-N,N'-bis(phenyl)benzidine, 99.95% purity, Gracel), Alq_3 (Tris(8-quinolinolato) aluminum, 99.9% purity, Gracel), and rubrene (99.96% purity, Gracel) were dissolved in a previously prepared solution of polystyrene (Mw: 280,000, Aldrich) in chloroform. The weight ratio of NPB, Alq_3, and rubrene dissolved in the chloroform were fixed through all experiments to be 1.0 : 1.0 : 0.15. The polystyrene was dissolved in the 50 ml chloroform as a host polymer in order to adjust the viscosity of the coating solution. For spin coating, 0.4 g of polystyrene was dissolved in the solvent. At the viscosity, the resulting film thickness was about 100 nm when the solution was spin-coated by two steps (2,000 rpm for 5 sec and 4,000 rpm for 60 sec). In order to prepare the film of same composition and thickness by using screen printing, 0.8 g of polystyrene was dissolved in the same amount of solvent and the solution was screen-printed using 400 mesh stainless steel screen mask. The coating solution was filtered through a 0.20 μm PTFE syringe filter right before the spin coating and screen printing. The OLED area was 25 mm×25 mm (49 pixels) and a pixel size was 3 mm×3 mm.

The average thickness of the organic film, measured with a KLA Tencor alpha-step, was about 100 nm. An LiF layer of 0.5 nm and an Al layer of 120 nm thickness were successively deposited in the same chamber on top of the printed organic layer under 5×10^{-7} torr pressure.

RESULTS AND DISCUSSION

In order to ensure the thickness of a polymer film to be less than 100 nm as the result of spin coating and screen printing, the viscos-

†To whom correspondence should be addressed.
E-mail: sungmcho@skku.edu

ity of the coating solutions should be strictly controlled. Not only does the viscosity of the coating solutions affect the resulting film thickness, but also the process conditions of coating such as the spin speed, mesh counts, coating time, *etc*. have significant influence on it. In the case of all the process conditions to be fixed other than solution viscosity, the solution viscosity for spin coating should be lower than that for screen printing to result in the same thickness. Fig. 1 shows the resulting film thickness for screen printing with the solutions of various polystyrene contents in 50 ml chloroform. When 0.8 g polystyrene was dissolved in 50 ml chloroform, the solution produced a polystyrene film of thickness about 100 nm as the result of screen printing with 400 mesh screen as shown in Fig. 1. In order for a polymer film to be used for OLED emissive layer, the film thickness should be less than 100 nm. In this study, therefore, the screen printing has been always carried out with a solution composition of 0.8 g PS/50 ml chloroform. With the conditions of spin coating described in the experimental section, the solution composition of 0.4 g PS/50 ml chloroform has been found to be the optimal composition for producing the PS film of the same thickness. It should be mentioned here that the addition of low-molecular-weight organic molecules such as NPB, Alq_3, and rubrene did not affect the solution viscosity significantly. Throughout this study, all the coating solutions were prepared to have a weight ratio of NPB : Alq_3 : rubrene to be 1.0 : 1.0 : 1.5, regardless of spin coating and screen printing.

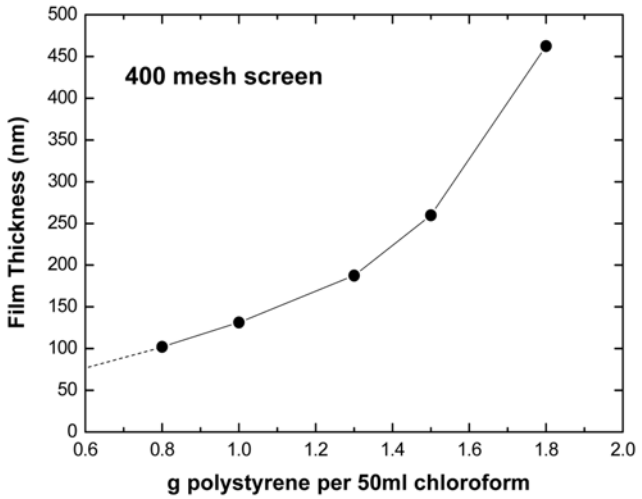

Fig. 1. The resulting thickness of screen-printed films with respect to the polystyrene content in 50 ml chloroform solvent.

The surface morphology of the screen-printed organic film was found to be greatly affected by the surface condition of the substrate. When the PS-based coating solution was screen-printed on bare glass or ITO surface, the screen printing was found to leave many pinholes behind in the resulting films as shown in Fig. 2.

Spreading coefficient S as a factor determining the wetting and dewetting is usually defined to be $S=S_E-F_E-SF_E$, where S_E and F_E are the surface energies of the substrate and film on the substrate, respectively. And, SF_E is the interfacial energy between film and substrate. When $S>0$, the surface is considered wettable, and if $S<0$, dewetting occurs. Wetting and dewetting are important processes for many applications, including adhesion, lubrication, painting, printing, and protective coating. Untreated bare glass and ITO are known to have the contact angles around 50-60°. A surface treatment using oxygen plasma usually gives rise to the reduction of

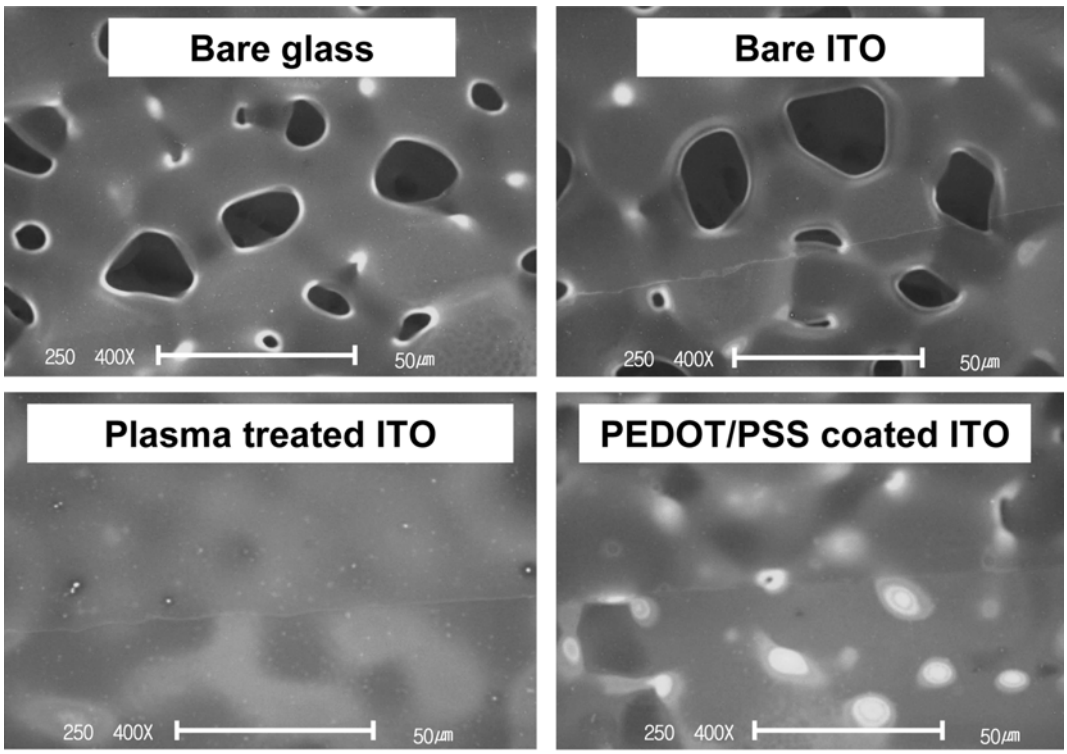

Fig. 2. Photographs showing the surface morphology of the screen-printed films deposited on the differently treated substrates.

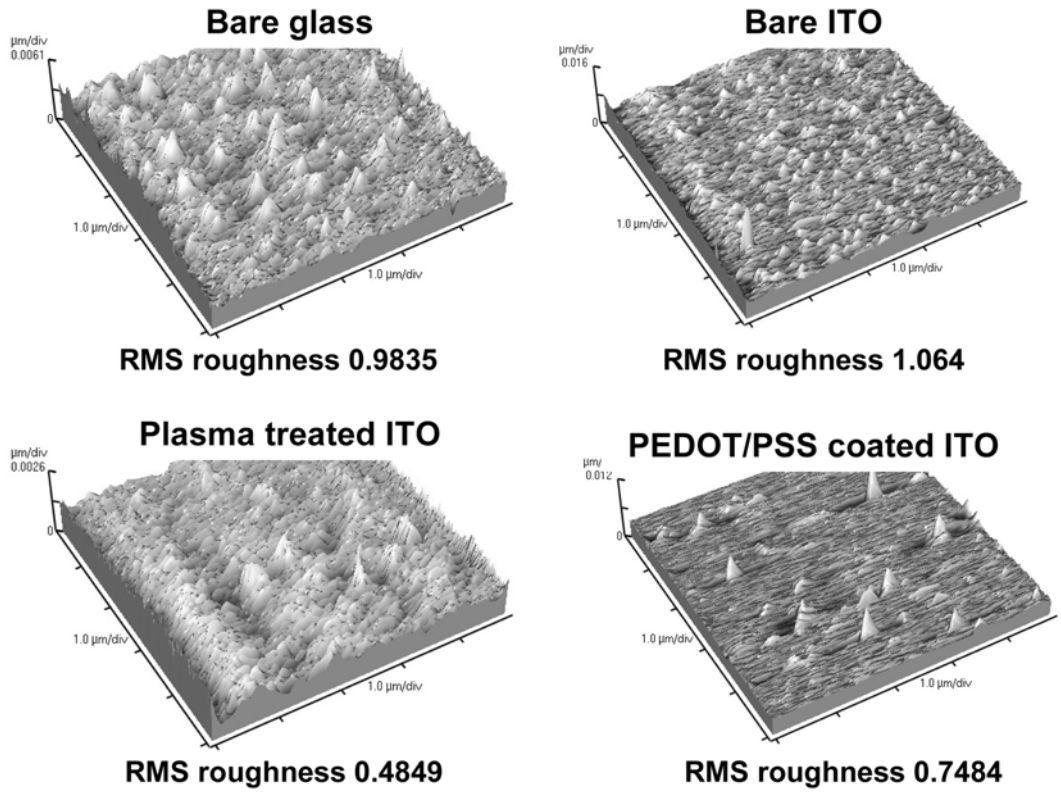

Fig. 3. AFM images showing the r.m.s. roughness of the screen-printed films deposited on the differently treated substrates.

contact angle to less than 20°. The contact angle of water on the PEDOT/PSS surface is measured to be less than 10°. Since more hydrophilic surfaces have lower contact angles and higher surface energies, the oxygen plasma treatment and PEDOT/PSS coating should enhance wetting of the printed film. As shown in Fig. 2, the polystyrene films printed on the bare glass and ITO display a number of pinholes of size ranging from a few to few tens micrometer. It could be understood that the pinholes have been created due to dewetting of hydrophobic polystyrene on the bare glass and ITO surfaces. Upon the oxygen plasma treatment or the coating of PEDOT/PSS of ITO substrates, the dewetting is reduced remarkably because of the increase in hydrophilicity of the ITO substrate, which means higher surface energy of the substrate.

The surface roughness depends directly on the surface morphology produced by the wetting and dewetting. As shown in Fig. 3, the root mean square (rms) roughness of the films screen-printed on the bare glass and ITO was measured to be 0.98 and 1.06 nm, respectively. It is because there are a number of pinholes on the surfaces. As expected, for the organic films screen-printed on the plasma-treated and PEDOT/PSS-coated ITO surfaces, the r.m.s. roughness was measured to be 0.48 and 0.74 nm, respectively, which was much lower compared with that of the films on bare glass and ITO surfaces.

We have fabricated single-layer OLEDs using the screen-printed organic films. For comparison, OLEDs of the same structure have been also fabricated by using spin coating. In order to adjust the thickness of the organic films prepared by the spin coating and screen printing to be the same as 100 nm, the polystyrene content of the spin-coating solution had to be reduced to half of that for the screen printing, as mentioned earlier. The hole transporting (NPB), electron transporting (Alq_3), and emitting (rubrene) organic materials were added when the coating solutions were prepared. The weight ratio of NPB, Alq_3, and rubrene was fixed to 1.0 : 1.0 : 0.15, which was optimized by way of measuring the brightness of OLEDs fabricated by the spin coating. The OLED fabricated by the spin coating was turned on at 10 V and reached a maximum brightness of 1,100 Cd/m^2 at 21 V. On the contrary, the OLED fabricated by screen printing showed the same turn-on voltage and the maximum brightness of

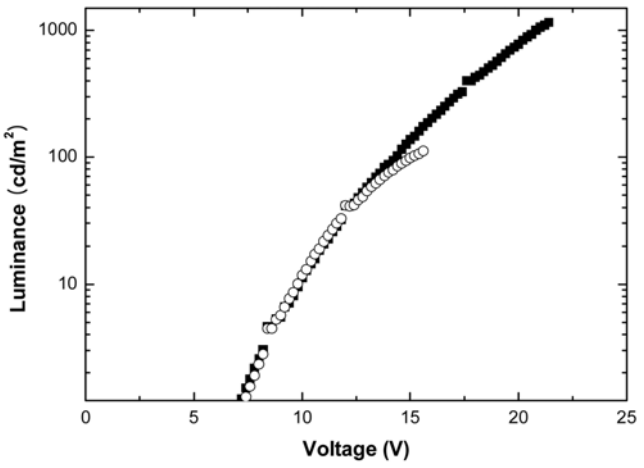

Fig. 4. Brightness of screen-printed (open symbol) and spin-coated (filled symbol) OLEDs with respect to the operating voltage.

110 Cd/m^2 at 14 V. The voltage-luminance curve is shown in Fig. 4. The reason why the screen-printed OLED showed the inferior performance is presumed to be due to the inferior quality of organic thin film. Even though the creation of pinholes has been suppressed greatly by the surface treatments of substrates, the resulting organic films have been still inferior to those obtained from spin coating. It should be also mentioned that the emission from the screen-printed OLEDs was not perfectly uniform but rather scattered as innumerable tiny emitting dots throughout the device area. From this observation, we could conclude that the emitting dyes were not uniformly dispersed in the PS layer for some reasons. We attribute this non-uniform dispersion to the pinholes still present in the organic film. Even though the pinholes have been suppressed by the surface treatments of the substrate, it is expected that the pinholes could still exist in the organic film and the aggregation of emitting dyes could have been facilitated by the non-uniform drying during the creation of pinholes. In order to investigate the non-uniform emission of the screen-printed OLEDs further, we have observed the OLED degradation behavior and the dark spot generation.

Burrows et al. [10] thoroughly investigated the formation of dark spots in OLEDs and suggested that these formations were a result of high current areas in the device. Once formed, dark spots increase in size leading to total device failure. Antoniadis et al. [11] also investigated the degradation mechanisms involved in OLEDs. They proposed that dark spots are pinholes in the cathode material in which water and oxygen can enter the device and affect the organic molecules. Particles and other imperfections existing on the ITO surface or introduced during device fabrication are prime candidates for pinhole formation.

As shown in Fig. 5, the degradation behavior of the OLED fabricated by the spin coating, which is the bottom series of pictures in the figure, exhibits the dark spots. In the micrographs, the black area represents emission, while a white or gray area represents the dark spots. The dark spots began appearing during emission, and as time passed they grew bigger along with the creation of new dark spots. However, the degradation behaviors of the OLEDs fabricated by the screen printing could be characterized to exhibit the abrupt creations of big dark spots until the OLEDs completely failed. As can be seen in the figure, the dark spots for the screen-printed OLED on the untreated ITO substrate seem to be unchanged after a few dark spots were created. It means that the OLEDs have completely failed. However, the screen-printed OLEDs on the plasma-treated or PEDOT/PSS-coated ITO substrate seem to live much longer even though more dark spots have already been created. It can be understood that the OLEDs fabricated by the screen printing on untreated ITO substrate have many pinholes on the surface and the pinholes may act as points where the electrical shorts occur. Even though the screen-printed OLEDs on the surface-treated ITO substrates live longer than those on untreated ITO substrate, the size of dark spots is found to be much bigger compared with the case of the OLEDs fabricated by the spin coating. It can be attributed to the fact that the emitting dyes in the screen-printed OLEDs should have not been dispersed uniformly but aggregated in areas unlike the case of the spin-coated OLEDs. We presume that the non-uniformity of dye dispersion has been caused by the pinholes or non-uniform drying of surface. In order to improve the performance of the screen-printed OLEDs close to that of the spin-coated OLEDs, it is important to have the organic thin film to be dried more uniformly while keeping the surface pinhole-free.

CONCLUSIONS

Single-layer OLEDs have been fabricated by the screen printing method and their device performance has been compared with the

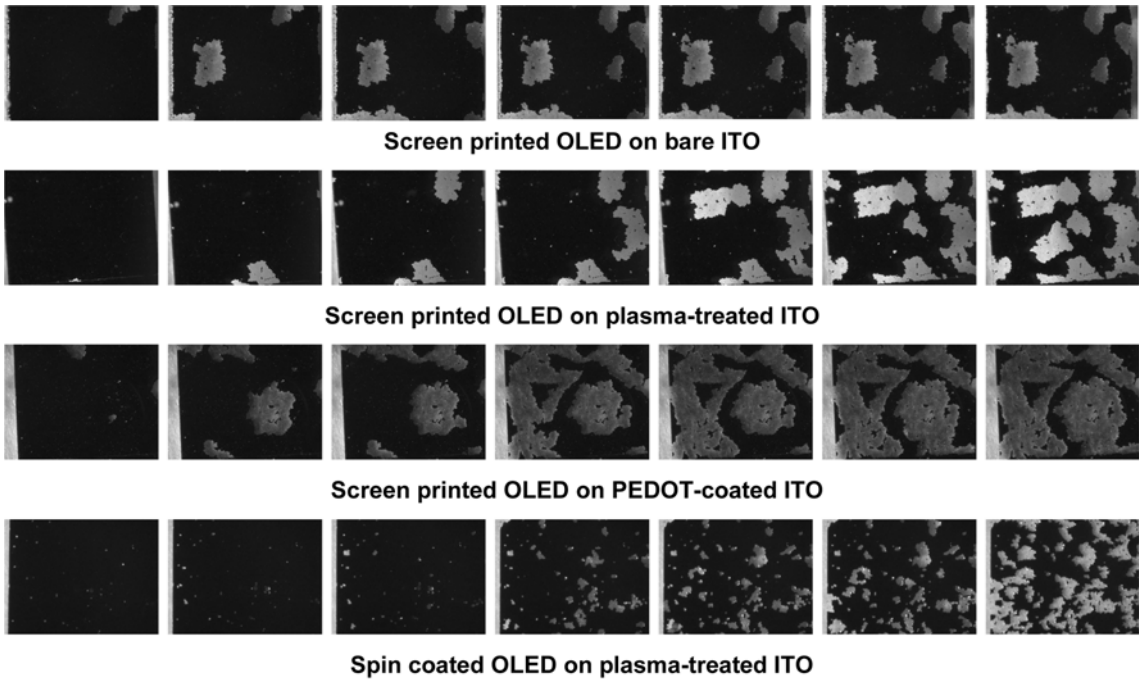

Fig. 5. Photographs showing the degradation of screen-printed and spin-coated OLEDs.

single-layer OLEDs fabricated by spin coating. We have shown that it is possible to deposit a 100 nm-thick organic film by screen printing and the film can be used to fabricate the single-layer OLEDs. It has been found that the oxygen plasma treatment or PEDOT/PSS coating of ITO substrate surface could suppress the creation of pinholes by reducing the dewetting. At this stage of research, even though the brightness of the screen-printed OLEDs is only slightly above 100cd/m^2 and the emission is not perfectly uniform, it is expected that the performance of the screen-printed OLEDs can be improved further by the optimization of materials used and process conditions.

ACKNOWLEDGMENTS

This work was partly supported by the 'Local Government Initiated R&D Program (Project No. 2004-0693-100)' of the Korea Ministry of Commerce, Industry and Energy accompanying with the Gyeonggi Province and also supported in part by Grant No. (R01-2006-000-10140-0) from the Basic Research Program of the Korea Science & Engineering Foundation.

REFERENCES

1. J. Kim, M. Song, J. Seol, H. Hwang and C. Park, *Korean J. Chem. Eng.*, **22**, 643 (2005).
2. V.-E. Choong, J. Shen, J. Curless, S. Shi, J. Yang and F. So, *J. Phys. D: Appl. Phys.*, **33**, 760 (2000).
3. J. P. J. Markham, S.-C. Lo, S. W. Magennis, P. L. Burn and I. D. W. Samuel, *Appl. Phys. Lett.*, **80**, 2645 (2002).
4. Y. Zhang, Y. Hu, J. Chen, Q. Zhou and D. Ma, *J. Phys. D: Appl. Phys.*, **36**, 2006 (2003).
5. Y.-H. Niu, B. Chen, T.-D. Kim, M. S. Liu and A. K.-Y. Jen, *Appl. Phys. Lett.*, **85**, 5433 (2004).
6. X. Gong, S.-H. Lim, J. C. Ostrowski, D. Moses, C. J. Bardeen and G. C. Bazan, *J. Appl. Phys.*, **95**, 948 (2004).
7. H. Xia, C. Zhang, S. Qiu, P. Lu, J. Zhang and Y. Ma, *Appl. Phys. Lett.*, **84**, 290 (2004).
8. D. A. Pardo, G. E. Jabbour and N. Peyghambarian, *Adv. Mater.*, **12**, 1249 (2000).
9. G. E. Jabbour, R. Radspinner and N. Peyghambarian, *IEEE J. Sel. Top. Quant. Elect.*, **7**, 769 (2001).
10. P. E. Burrows, V. Bulovic, S. R. Forrest, L. S. Sapochak, D. M. McCarty and M. E. Thompson, *Appl. Phys. Lett.*, **65**, 2922 (1994).
11. H. Antoniadis, M. R. Hueschen, J. N. Miller, R. L. Moon, D. B. Roitman and J. R. Sheats, *Macromol. Symp.*, **125**, 59 (1997).